

Synthesis of 11 Å Al-substituted tobermorite from trachyte rock by hydrothermal treatment

H. Youssef^a, D. Ibrahim^a, S. Komarneni^{b,*}, K.J.D. Mackenzie^c

^a National Research Centre, Department of Ceramics, Refractories and Building Materials, El Behos St. Dokki, 12622 Cairo, Egypt

^b Materials Research Institute and Department of Crop and Soil Sciences, 205 Materials Research Laboratory, The Pennsylvania State University, University Park, PA 16802, USA

^c School of Chemical and Physical Sciences, Victoria University of Wellington, P.O. Box 600 Wellington, New Zealand

Received 6 May 2009; received in revised form 20 June 2009; accepted 12 July 2009

Available online 11 August 2009

Abstract

The alkaline hydrothermal activation of trachyte rock led to synthesis of technologically important 11 Å tobermorite. Tobermorite synthesis was studied by X-ray diffraction, scanning electron microscopy and ²⁹Si and ²⁷Al high resolution magic angle spinning nuclear magnetic resonance (MAS-NMR) spectroscopy. The influence of the reaction conditions such as different temperatures (150–170 °C), times (5–20 h) as well as different Ca/Si ratios of 0.6, 0.9 and 1.3 on tobermorite formation were investigated. The results showed that the main rock constituents were completely converted into a well crystallized Al-substituted 11 Å tobermorite when hydrothermally activated with 3.0 M NaOH under the optimum hydrothermal conditions of 170 °C for 20 h and using Ca/Si and Al/Al + Si ratios of 0.9 and 0.17, respectively. The local structure of the synthesized tobermorites as determined by MAS-NMR spectroscopy implied an alumino-silicate mean chain length of 5.9 units with 79% of the interlayer cross-links which are of ≡Si–O–Al≡ configuration. The present results show that trachyte rock could be considered as a new economic resource for synthesizing Al-substituted 11 Å tobermorites.

© 2009 Elsevier Ltd and Techna Group S.r.l. All rights reserved.

Keywords: Al-substituted tobermorite; Trachyte; Hydrothermal synthesis; ²⁹Si and ²⁷Al MAS-NMR spectroscopy

1. Introduction

Tobermorites are layered calcium silicate hydrate minerals with an ideal $\text{Ca}_5\text{Si}_6\text{O}_{18}\text{H}_2\cdot 4\text{H}_2\text{O}$ composition [1]. Natural tobermorites are found as veins or filling amygdaloids in hyper-alkaline, hydrothermal environments as the alteration products of basic igneous rocks by hydrothermal fluids [2,3]. Tobermorites are commonly used as autoclaved concretes, which serve as non-asbestos, heat insulating and fire-resistant building materials as well as adsorbents for organic or inorganic effluents [4,5]. They can also be used as cation exchangers in the decontamination of radioactive species from low-level nuclear wastes [6–12]. Synthetic tobermorites have been discovered by Komarneni et al. [9] and Komarneni and Roy [13] as a new family of cation exchangers with an intermediate

cation exchange and selectivity properties between those of clays and zeolites. The coupled substitution of $[\text{Al}^{3+} + \text{Na}^+]$ or $[\text{Fe}^{3+} + \text{Na}^+]$ for Si^{4+} in the synthetic forms results in selective ion exchange properties for heavy metals such as Cd^{2+} , Pb^{2+} , Co^{2+} , Ni^{2+} and Cs^+ from aqueous solutions [7,9] that are superior to zeolites.

The natural, orthorhombic, rarely monoclinic 11 Å tobermorite is the most technologically important mineral of the tobermorite family [2,14]. Its ideal layer structure consists of an infinite layer of seven-coordinated Ca–O polyhedra linked on both sides to wollastonite-like silicate chains in an arrangement parallel to the *b*-axis, and stacked in the *c*-axis direction (Fig. 1) [15]. The vicinity of the interlayer forms a channel running along the *b*-axis direction where exchangeable calcium ions and water molecules are accommodated [16–19]. Tobermorite minerals are named according to their *c*-axis length which mainly depends on the number of water molecules per formula unit. Accordingly, the approximate *d*-spacing of the (0 0 2) Bragg reflection (i.e. the basal spacing) of 11 Å tobermorite lies

* Corresponding author. Tel.: +1 814 865 1542; fax: +1 814 865 2326.

E-mail address: Komarneni@psu.edu (S. Komarneni).

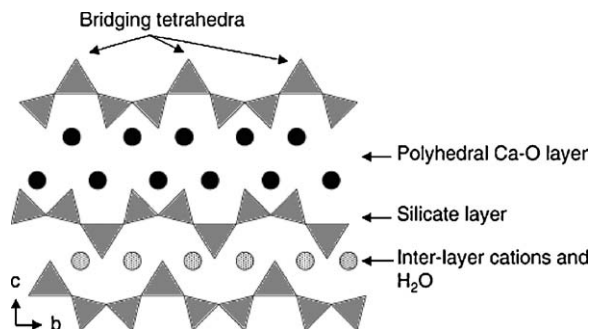


Fig. 1. Structural projection of 11 Å tobermorite in the *bc*-plane, showing the dreierkette chains of tobermorite where the silicate tetrahedra share O–O edges with the central Ca–O layer [15].

in the range of 11.2–11.7 Å. The deviation from the ideal structure is due either to breaks in the silicate chains which cause extensive layer stacking, or due to some compositional variation such as the coupled isomorphous replacement of up to 15% Al^{3+} for Si^{4+} with spontaneous OH^- for O^{2-} substitution and/or additional interlayer calcium or alkali ions [7,8,20–22].

Natural tobermorites are usually more highly crystalline than synthetic ones; however, their rare occurrence is the main reason for the production of synthetic alternatives. Synthetic 11 Å tobermorites and their Al- and Fe-substituted forms have been readily synthesized under saturated steam or hydrothermal conditions at temperatures between 80 and 225 °C from a range of starting materials including various mixtures of the following: lime, zeolites, quartz, gibbsite, cement, clays, fly ash, sodium silicate and aluminum chloride; and more recently, a number of industrial by-products [7,21,23,24]. Al-substituted 11 Å tobermorite has been synthesized from newsprint recycling residue comprising gehlenite ($\text{Ca}_2\text{Al}_2\text{SiO}_7$), akermanite ($\text{Ca}_2\text{MgSi}_2\text{O}_7$), β -dicalcium silicate (Ca_2SiO_4) and anorthite ($\text{CaAl}_2\text{Si}_2\text{O}_8$) under hydrothermal conditions at 100 °C for 1–2 days in the presence of NaOH [23,25]. In a recent study, hydrothermal alkaline activation of oil shale fly ash converted it to mainly 11 Å tobermorite after 24 h treatment under hydrothermal conditions at 160 °C in the presence of NaOH. Tobermorite fibers 40–100 μm in length and 0.1–1 μm in diameter were hydrothermally synthesized at 200 °C for 5 h, using a solution containing silicate ions and Ca(II)–EDTA complex precursor [26]. The starting Ca/Si molar ratio did not greatly influence the phase and morphology of tobermorite but determined its final composition.

Recently microwave heating has been used in tobermorite synthesis to increase the kinetics of crystallization [12]. A highly crystalline Al-substituted tobermorite with high cesium ion selectivity was rapidly synthesized in 2 h at 180 °C under microwave heating, from two zeolites (natural phillipsite and Linde 3A zeolite), calcium oxide, sodium silicate, aluminum chloride and sodium hydroxide.

As mentioned above, there is a notable relation between basic volcanic rocks and the formation of natural tobermorites [27]. Therefore, natural rocks with their great economic potential were used in this work to reduce the cost of production by substituting them for chemical reagents in the synthesis of tobermorites. Tobermorite synthesis as proposed in this paper refers to mineral

crystallization by a facile chemical treatment of natural alkali aluminosilicates derived by direct alkali-solution hydrothermal treatment of an inexpensive alkali volcanic rock (trachyte). Trachyte rocks are a group of fine-grained, generally porphyritic, extrusive igneous rocks consisting of alkali feldspar (usually sanidine) and minor mafic minerals as the main components, and possibly a small amount of sodic plagioclase [28].

2. Experimental

2.1. Chemicals and materials

The trachyte was supplied as igneous extrusive hand specimens (Ward's Catalog Reference #47-8273) by Ward's Natural Science Establishment, Inc., Rochester, NY, USA. The other chemicals used in the synthesis were NaOH pellets (Baker analyzed ACS reagent grade, 98.6% NaOH + 0.4% chloride), and ACS reagent grade $\text{Ca}(\text{OH})_2$, 98+% (Aldrich Chemical Company, Inc.).

2.2. Synthesis

Fig. 2 shows the flow chart for tobermorite synthesis from trachyte. The trachyte powder of particle size <63 μm was treated with 3.0 and 5.0 M NaOH solutions. The calculated amount of calcium hydroxide was then added, based on the Ca/Si ratio of the C–S–H formula of tobermorite. The batch constituents were stirred for 30 min to form the raw slurry (RS) used to obtain the tobermorite phase. This slurry was placed in a 125 ml Parr-type vessel lined with Teflon and heated at temperatures between 150 and 170 °C for times of 5–20 h. The solid product was collected, washed with distilled water, centrifuged several times and dried overnight for phase characterization.

2.3. Characterization

The chemical composition of trachyte was measured by X-ray fluorescence (XRF) using an AXIOS WD-XRF Sequential Spectrometer (Panalytical, 2005). The end window Rhodium (Rh) anode tube was operated at up to 60 kV and current up to 160 mA at a maximum power level of 4 kW. Phase identification was carried out by XRD Scintag diffractometer; model XDS 2000 with Ni-filtered Cu $K\alpha$ radiation. The patterns of all synthesized phases were recorded in the range of 4–45° 2θ and compared to the following JCPDS data base reference cards; 97-045-1480, 97-007-3393 and 97-004-0315 for 11 Å tobermorite [$\text{Ca}_5\text{Si}_6(\text{O},\text{OH},\text{F})_{18}\cdot 5\text{H}_2\text{O}$], Al-substituted tobermorite [$\text{Ca}_{4.9}(\text{Si}_{5.5}\text{Al}_{0.5}\text{O}_{16.3})(\text{OH})_{0.7}(\text{H}_2\text{O})_5$] and sodalite [$\text{Na}_8(\text{Al}_6\text{Si}_6\text{O}_{24})$], respectively. The morphology and particle size was observed by scanning electron microscopy, Philips XL30 with an attached EDX unit, using an accelerating voltage of 30 kV, magnification 10 \times up to 400,000 \times and resolution for W (3.5 nm). The ^{27}Al and ^{29}Si MAS-NMR (magic angle spinning nuclear magnetic resonance) spectra were acquired at 11.7 T using a Bruker Avance 500 spectrometer and 4 and 5 mm Doty MAS probes spun at 10–12 kHz for Al and 6 kHz for Si. A 1 μs

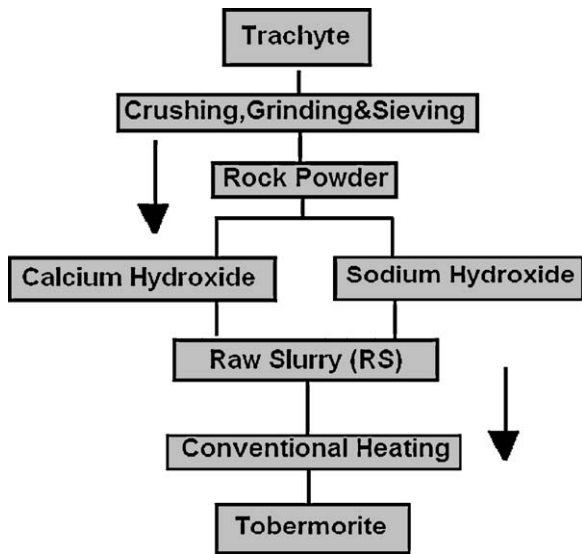


Fig. 2. Flow chart of the tobermorite synthesis from trachyte rock powder.

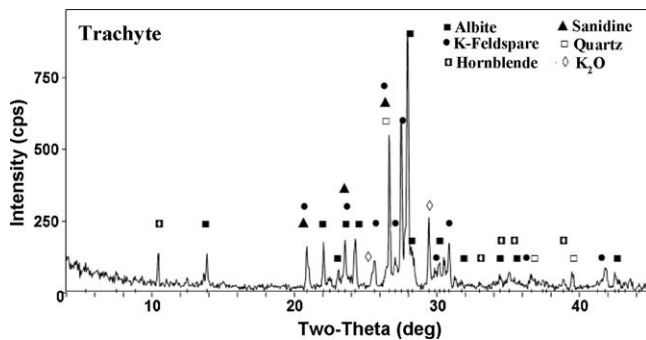


Fig. 3. XRD pattern of the mineralogical composition of trachyte rock powder.

($\pi/10$) pulse for solution with a 1 s delay was used for ^{27}Al and a 6 μs ($\pi/10$) pulse with a 30 s delay was used for ^{29}Si .

3. Results and discussion

The XRF results show that the trachyte consists of 62.03 wt% SiO_2 , 15.8 wt% Al_2O_3 , 8.37 wt% Fe_2O_3 , 4.86 wt% CaO , 3.96 wt% K_2O and 2.59 wt% Na_2O . Its mineralogical composition is shown in the XRD pattern (Fig. 3).

3.1. Effect of synthesis temperature

Table 1 shows the mineral assemblage occurring in the synthetic product formed at different temperatures and times,

and Figs. 4 and 5 show the XRD patterns of these phases and their SEM microstructures, respectively. The XRD results for the alkaline activated trachytes show no evidence of the presence of the original parent phases, especially in samples heated at 170 °C (Figs. 4c and 5c). However, the products obtained at 150 and 160 °C show lower intensities for the tobermorite peaks, as well as the presence of other interfering phases (Figs. 4a and b and 5a and b).

The SEM results show some unreacted rock components (feldspar and hornblende) as well as some unreacted portlandite, $\text{Ca}(\text{OH})_2$ in the final product. The SEM micrographs (Fig. 5) show that the higher temperature not only affected the product mineral phase assembly but also improved the crystal morphology of the tobermorite, which was transformed at increasing temperature from fibrous to prismatic and finally lath-like shaped grains in the samples treated at 150, 160 and 170 °C respectively (Fig. 5). Tobermorite, feldspar, portlandite, sodalite and cancrinite crystals in SEM pictures were identified by their platy, prismatic, hexagonal, hexagonal prisms and cubic morphology, respectively.

3.2. Effect of Ca/Si ratio

Figs. 6 and 7 and Table 2 show the effect of $\text{Ca}(\text{OH})_2$ additions in terms of the calculated Ca/Si ratio based on the given values of CaO and SiO_2 mol% of the trachyte composition and the Ca/Si ratios of literature values of tobermorite C–S–H formulae. Both low and high Ca/Si ratios resulted in fine tobermorite laths with relatively low peak intensities together with significant amounts of unreacted rock relicts (feldspar), some sodalite and cancrinite grains (Fig. 7a), as well as some unreacted plate-shaped portlandite (Fig. 7c).

From these results it is clear that alkali-hydrothermal treatment of trachyte powder yields 11 Å tobermorite as the main product when activation is conducted with 3.0 M NaOH at the three tested temperatures and Ca/Si ratios after 10–20 h of treatment. However, the tobermorite is accompanied by some impurity phases. At lower temperatures and/or time, the presence of rock constituents (Hb and Feld) in the final product indicates sluggish dissolution of the main components that contribute to tobermorite formation. This explains the slow rate of tobermorite formation reflected in its low peak intensities, low crystallinity and low % yield at lower temperature and/or times. The calcium deficiency caused by partial reaction of the added $\text{Ca}(\text{OH})_2$, as indicated by the presence of portlandite, also contributes to this delay. Moreover, the dissolution reaction might have occurred over an extended time and/or higher

Table 1
Mineral phases detected in the synthetic product at different temperatures and durations.

Time (h)	Temperature (°C)		
	150	160	170
5	Feld + TOB + Port + Hb + SOD	Feld + TOB + Hb + Port + SOD	TOB + SOD
10	TOB + Feld + Hb + Port + SOD	TOB + Hb + feld + Port + SOD	TOB + SOD
20	TOB + Feld + Port + SOD	TOB + Hb + Port + SOD	TOB + SOD

Feld = feldspar; TOB = tobermorite; Port = portlandite; Hb = hornblende; SOD = sodalite.

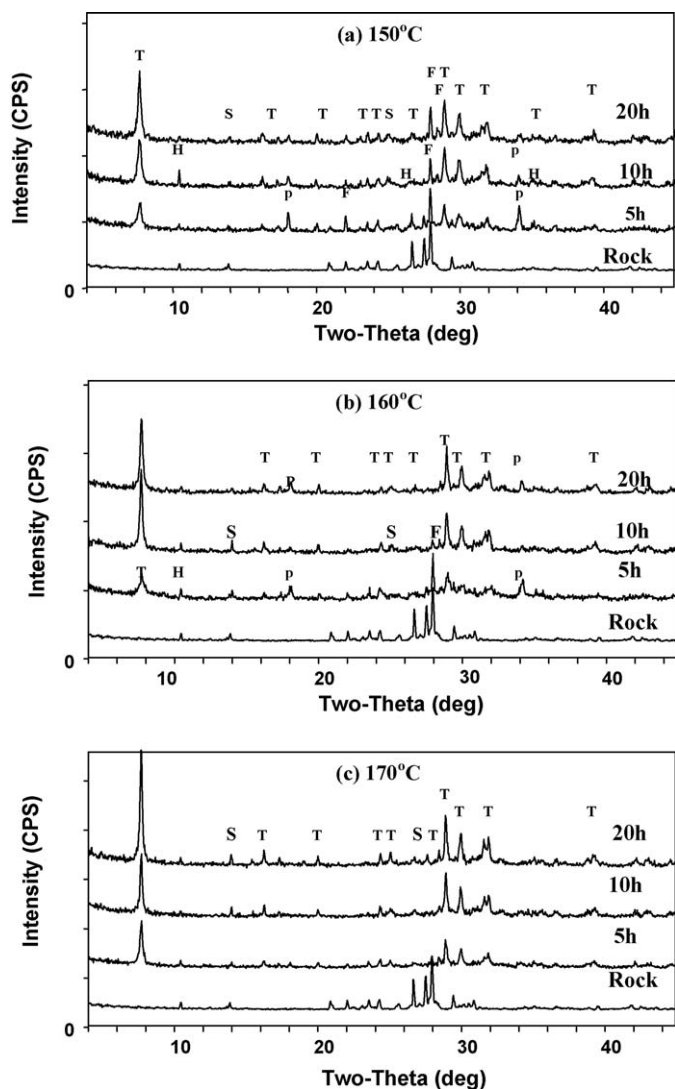


Fig. 4. XRD patterns showing the temperature effect on tobermorite developed from trachyte rock powder treated with 3.0 M NaOH for different durations at temperatures of (a) 150 °C, (b) 160 °C and (c) 170 °C. T = tobermorite; F = feldspar; P = portlandite; H = hornblende; S = sodalite.

temperature. By contrast, at 170 °C using a Ca/Si ratio of 0.9, a well developed and purer tobermorite mineral was formed with the highest % yield and peak intensity, accompanied by very low sodalite peak intensities. The development of sodalite in the system is the direct expression of the high alkalinity of the medium [29,30].

3.3. MAS-NMR results

One of the most significant methods to provide information about the types and structures of the silicate anions in the tobermorite structure is MAS-NMR spectroscopy. This method makes it possible to selectively determine the individual SiO_4 structural units in the synthetic tobermorite.

The ^{29}Si MAS-NMR spectrum shown in Fig. 8 contains a resonance at about -85 ppm, assigned to the mid-chain Q^2 silicate tetrahedra of the wollastonite-like alumino-silicate chains [7,31,32]. The presence of the branching sites $Q^3(1\text{Al})$

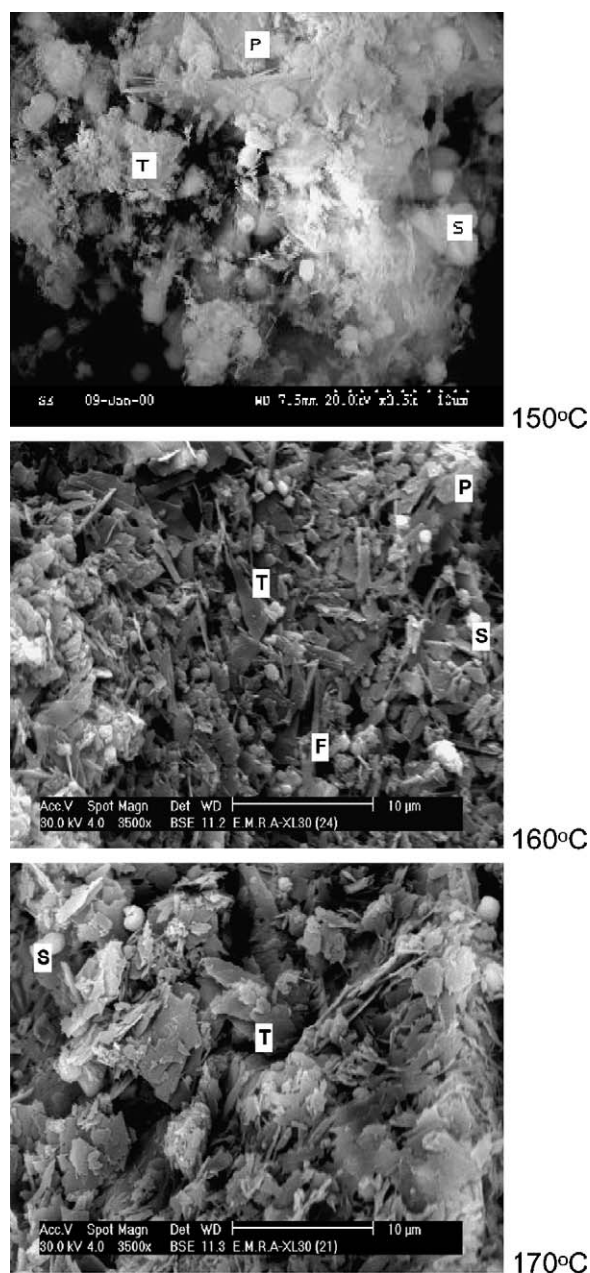


Fig. 5. SEM micrographs show the effect of different temperatures on the mineral phases and tobermorite morphology. T = tobermorite; F = feldspar; P = portlandite; S = sodalite.

and Q^3 is indicative of the bridging silicate tetrahedra which cross-link two silicate chains. Generally, the presence of Q^2 and Q^3 shows that this sample contains a double-chain structure of silicate anions, which agrees with the results of previous NMR observations of 1.1 nm tobermorites [9,13,31,33] and with the reported crystal structure [18,19]. Moreover, the signal from $Q^3(1\text{Al})$ is shifted to higher frequency by Al substitution [7], indicating that the Al substitutes for Si in the bridging sites. The Q^1 signal represents the end group of a chain structure or a dimer [31,34], while Q^0 represents isolated silica tetrahedra, and Q^4 can be assigned to silica gel.

The ^{29}Si MAS-NMR data can be used to estimate some of the silicate chain parameters of the tobermorites by using semi

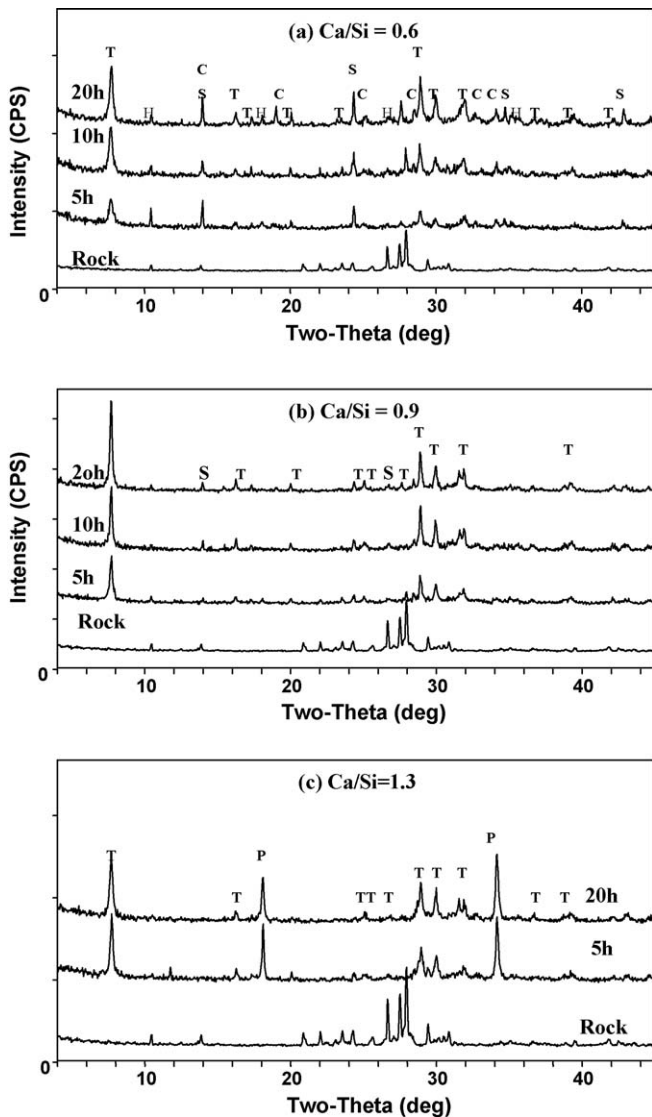


Fig. 6. XRD results of the effect of Ca/Si ratios on the mineral phases developed at 170 °C.

quantitative calculations, making the generally accepted assumption that essentially all the Al^{3+} -for- Si^{4+} substitution occurs at bridging positions [31].

This assumption was used to make a semiquantitative estimation of the relative ‘mean chain length’ (MCL) and ‘cross-linking quotient’ (CLQ) parameters. MCL is a measure of the average number of tetrahedra linked along the *b*-axis direction between breaks in the chain, whereas the CLQ can be

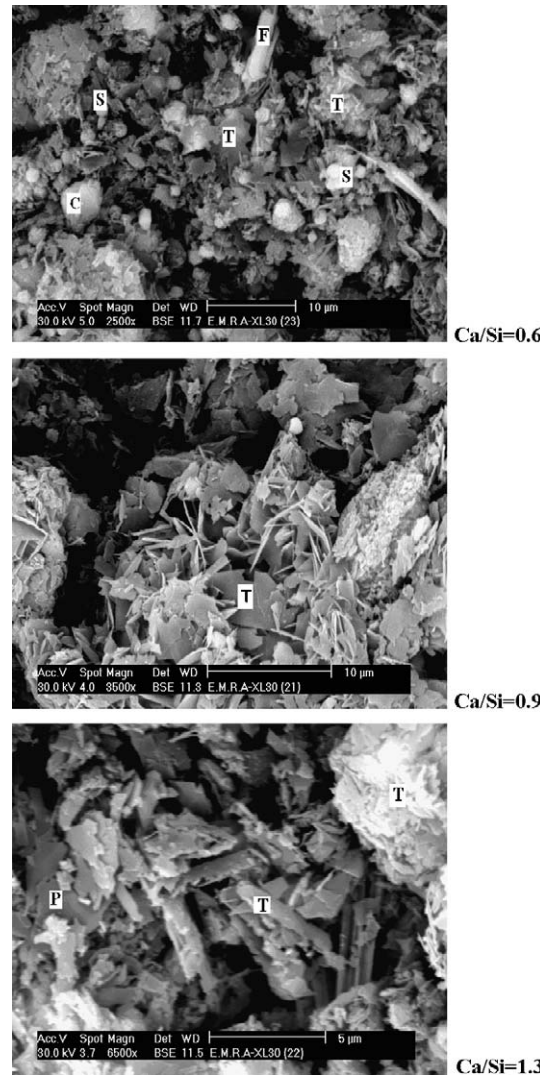


Fig. 7. SEM micrographs show the effect of $\text{Ca}(\text{OH})_2$ addition on tobermorite synthesis from trachyte powder treated with 3.0 M NaOH at 170 °C for 20 h. T = tobermorite; F = feldspar; P = portlandite; S = sodalite; C = cancrinite.

defined as the ratio of bridging tetrahedra which are condensed across the interlayer relative to the total number of tetrahedra. Both parameters are discussed in Ref. [15].

Analysis of the ^{29}Si MAS-NMR data indicates that the mean alumino-silicate chain length of the synthetic tobermorite is 5.9 units, and the linking quotient is 0.29. Therefore, nearly 89% of all bridging tetrahedra are condensed across the interlayer. Furthermore, comparison of the Q^3 and $\text{Q}^3(\text{Al})$ signal

Table 2
Mineral phases detected in the synthetic product at 170 °C with different $\text{Ca}(\text{OH})_2$ additions.

Time (h)	Ca/Si ratio		
	0.6	0.9	1.3
5	TOB (major) + minor (CAN + SOD + Hb)	TOB + SOD	TOB + Port
10	TOB (major) + more SOD + less CAN + Hb	TOB + ISOD (detected)	TOB + Port (detected)
20	TOB (major) + more SOD + more CAN + Hb	TOB + SOD (detected)	TOB + Port (detected)

TOB = tobermorite; CAN = cancrinite; Port = portlandite; Hb = hornblende; SOD = sodalite.

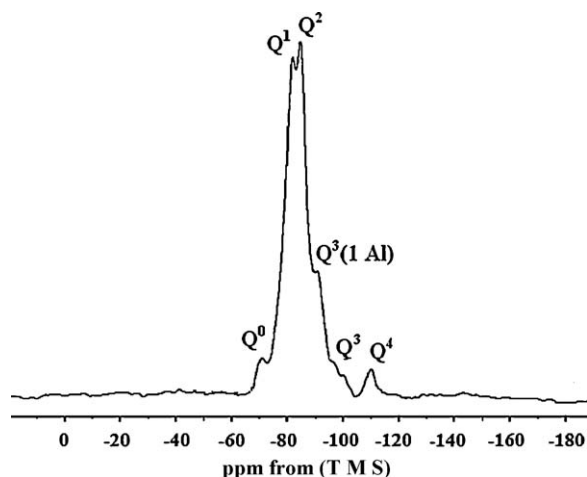


Fig. 8. ^{29}Si MAS-NMR spectrum of a tobermorite sample with 0.9 Ca/Si ratio, synthesized at 170 °C for 20 h.

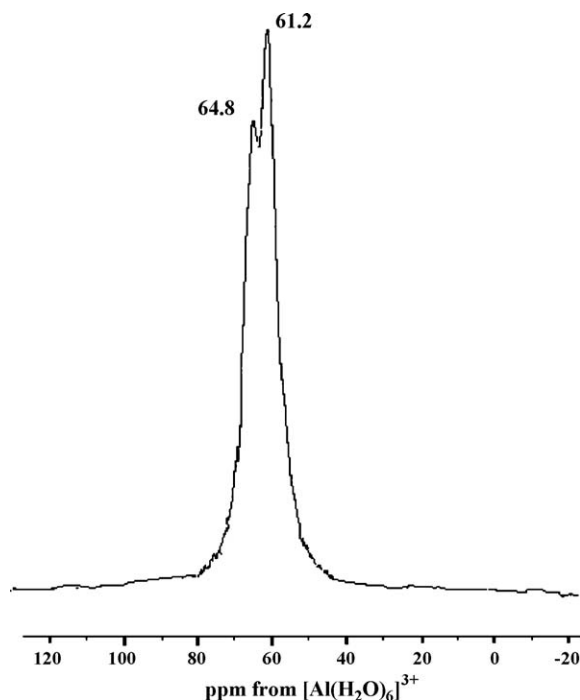


Fig. 9. ^{27}Al MAS-NMR spectrum of a tobermorite sample with 0.9 Ca/Si ratio, synthesized at 170 °C for 20 h.

intensities shows that about 79% of the interlayer cross-linkages are of a $\equiv\text{Si}-\text{O}-\text{Al}\equiv$ configuration, whereas the remaining 21% of the interlayer cross-linkages are of a $\equiv\text{Si}-\text{O}-\text{Si}\equiv$ configuration. The last finding is consistent with Loewenstein's rule which forbids the linkage of two tetrahedrally coordinated neighboring aluminum species via an oxygen atom [35].

Fig. 9 shows the ^{27}Al MAS-NMR spectrum of the synthetic product. The resonances at 61.2 and 64.8 ppm correspond well with those reported for pure Al-substituted 11 Å tobermorite [31,32]. The assignment of the two Al lines has been associated with the lattice substitution of Al for Si in two different environments, the 64.8 ppm resonance corresponding to substitution in the middle chain Q^2 and the 61.2 ppm resonance

to substitution in the bridging Q^3 sites [7,36,37]. The presence of $\text{Q}^3(1\text{Al})$ is consistent with the previous conclusion but the absence of a $\text{Q}^2(1\text{Al})$ signal is not. However, a $\text{Q}^2(1\text{Al})$ signal could be present under the broad envelope of the Q^1 peak at about -80 to -83 ppm [25].

4. Conclusion

Trachyte rock can be considered as an important new economic resource for the synthesis of Al-substituted 11 Å tobermorite. The optimum hydrothermal conditions for trachyte activation using 3.0 M NaOH were found to be 170 °C for 20 h using Ca/Si and Al/Al + Si ratios of 0.9 and 0.17, respectively. These synthetic Al-substituted tobermorites have potential uses as cation exchangers for the separation of radioactive and other hazardous cations.

Acknowledgments

The authors thank the Egyptian government, Scientific research Academy for financially supporting this study.

References

- [1] M.F. Heddle, Mineral. Mag. 4 (1980) 119–123.
- [2] C. Hoffman, T. Armbruster, Z. Kristallogr. 212 (1997) 864–873.
- [3] C. Henmi, I. Kusachi, Mineral. Mag. 56 (1992) 353–358.
- [4] P.G. Walter, United States Patent 4,128,434 (1978).
- [5] S. Kaneco, K. Itoh, H. Katsumata, T. Susuki, K. Masuyama, K. Funasaka, K. Hatano, K. Ohta, Environ. Sci. Technol. 37 (2003) 1448.
- [6] M. Miyake, S. Niiya, M. Matsuda, J. Mater. Res. 15 (2000) 850–853.
- [7] S. Komarneni, D.M. Roy, J. Mater. Sci. 20 (1985) 2930–2936.
- [8] M. Miyake, S. Komarneni, R. Roy, Mater. Res. Bull. 24 (1989) 311–320.
- [9] S. Komarneni, D.M. Roy, R. Roy, Cement Concrete Res. 12 (1982) 773–780.
- [10] M. Tsuji, S. Komarneni, J. Mater. Res. 4 (1989) 698–703.
- [11] O.P. Shrivastava, F.P. Glasser, React. Solids 2 (1986) 261–268.
- [12] S. Komarneni, J.S. Komarneni, B. Newalkar, S. Stout, Mater. Res. Bull. 37 (2002) 1025–1032.
- [13] S. Komarneni, D.M. Roy, Science 221 (1983) 647–648.
- [14] A. Athinson, A.W. Harris, J.A. Hearne, UK. Nirex Report NSS/R (1995) 374.
- [15] N.J. Coleman, Sep. Purif. Technol. 48 (2006) 62–70.
- [16] H.D. Megaw, C.H. Kelsey, Nature 177 (1956) 390–391.
- [17] S.A. Hamid, Z. Kristallogr. 154 (1981) 189–198.
- [18] S. Merlino, E. Bonaccorsi, T. Armbruster, Am. Mineral. 84 (1999) 1613–1621.
- [19] S. Merlino, E. Bonaccorsi, T. Armbruster, Eur. J. Mineral. 13 (2001) 577–590.
- [20] G.L. Kalousek, J. Am. Ceram. Soc. 40 (1957) 74–80.
- [21] S. Diamond, J.L. White, W.L. Dolch, Am. Mineral. 51 (1966) 388–401.
- [22] W. Nocun-Wezelik, Cement Concrete Res. 29 (1999) 1759–1767.
- [23] N.J. Coleman, D.S. Brassington, Mater. Res. Bull. 38 (2003) 485–497.
- [24] N.J. Coleman, Mater. Res. Bull. 40 (2005) 2000–2013.
- [25] J. Reinik, I. Heinmaa, J.-P. Mikkola, U. Kirso, Fuel 86 (2007) 669–676.
- [26] X. Huang, D. Jiang, S. Tan, J. Eur. Ceram. Soc. 23 (2003) 123–126.
- [27] A. Livingston, Mineral. Mag. 52 (1988) 711–713.
- [28] The Encyclopædia Britannica Eleventh Edition (1910–1911) is perhaps the most famous edition of the Encyclopædia Britannica.
- [29] M. Barns, J.A. Mensah, R.A. Gerson, Colloid Surf. A: Physicochem. Eng. Aspects 157 (1999) 101–116.
- [30] G. Hermeler, J.Ch. Buchl, W. Hoffmann, Catal. Today 8 (1991) 415.

- [31] W. Wieker, A.T. Grimmer, A. Winkler, M. Magi, M. Tarmak, E. Lippmaa, Cement Concrete Res. 12 (1982) 333–339.
- [32] R. Gabrovsek, B. Kurbus, D. Mueller, W. Wieker, Cement Concrete Res. 23 (1993) 321–328.
- [33] M. Sakiyama, T. Maeshima, T. Mitsuda, J. Soc. Inorg. Mater. Jpn. 7 (2000) 413–419.
- [34] Y. Okada, H. Ishida, T. Mitsuda, J. Am. Ceram. Soc. 77 (1994) 765–768.
- [35] W. Loewenstein, Am. Mineral. 39 (1954) 92–96.
- [36] P. Faucon, T. Charpentier, A. Nonat, J.C. Petit, J. Am. Chem. Soc. 120 (1998) 12075–12082.
- [37] J. Schneider, M.A. Cincotto, H. Panepucci, Cement Concrete Res. 31 (2001) 993–1001.